Available online at www.sciencedirect.com
ScienceDirect
Trans. Nonferrous Met. Soc. China 25(2015) 1325−1333
Transactions of Nonferrous Metals Society of China
www.tnmsc.cn

Behaviors of vanadium and chromium in coal-based direct reduction of high-chromium vanadium-bearing titanomagnetite concentrates followed by magnetic separation

Long-sheng ZHAO[1,2,3], Li-na WANG[2,3], De-sheng CHEN[2,3], Hong-xin ZHAO[2,3], Ya-hui LIU[2,3], Tao QI[2,3]

1. University of Chinese Academy of Sciences, Beijing 100049, China;
2. National Engineering Laboratory for Hydrometallurgical Cleaner Production Technology, Institute of Process Engineering, Chinese Academy of Sciences, Beijing 100190, China;
3. Key Laboratory of Green Process and Engineering, Institute of Process Engineering,Chinese Academy of Sciences, Beijing 100190, China

Received 15 March 2014; accepted 13 October 2014

Abstract: The reduction behaviors of $FeO{\cdot}V_2O_3$ and $FeO{\cdot}Cr_2O_3$ during coal-based direct reduction have a decisive impact on the efficient utilization of high-chromium vanadium-bearing titanomagnetite concentrates. The effects of molar ratio of C to Fe n(C)/n(Fe) and temperature on the behaviors of vanadium and chromium during direct reduction and magnetic separation were investigated. The reduced samples were characterized by X-ray diffraction (XRD), scanning election microscopy (SEM) and energy dispersive spectrometry (EDS) techniques. Experimental results indicate that the recoveries of vanadium and chromium rapidly increase from 10.0% and 9.6% to 45.3% and 74.3%, respectively, as the n(C)/n(Fe) increases from 0.8 to 1.4. At n(C)/n(Fe) of 0.8, the recoveries of vanadium and chromium are always lower than 10.0% in the whole temperature range of 1100−1250 °C. However, at n(C)/n(Fe) of 1.2, the recoveries of vanadium and chromium considerably increase from 17.8% and 33.8% to 42.4% and 76.0%, respectively, as the temperature increases from 1100 °C to 1250 °C. At n(C)/n(Fe) lower than 0.8, most of the $FeO{\cdot}V_2O_3$ and $FeO{\cdot}Cr_2O_3$ are not reduced to carbides because of the lack of carbonaceous reductants, and the temperature has little effect on the reduction behaviors of $FeO{\cdot}V_2O_3$ and $FeO{\cdot}Cr_2O_3$, resulting in very low recoveries of vanadium and chromium during magnetic separation. However, at higher n(C)/n(Fe), the reduction rates of $FeO{\cdot}V_2O_3$ and $FeO{\cdot}Cr_2O_3$ increase significatly because of the excess amount of carbonaceous reductants. Moreover, higher temperatures largely induce the reduction of $FeO{\cdot}V_2O_3$ and $FeO{\cdot}Cr_2O_3$ to carbides. The newly formed carbides are then dissolved in the γ(FCC) phase, and recovered accompanied with the metallic iron during magnetic separation.

Key words: high-chromium vanadium-bearing titanomagnetite concentrates; coal-based direct reduction; magnetic separation; reduction behavior; vanadium; chromium

1 Introduction

Panzhihua−Xichang (Panxi) region in China is widely recognized by large volumes of vanadium-bearing titanomagnetite, and the proven deposits of titanium and vanadium account for 35.2% and 11.6% of world total reserves, respectively [1]. Vanadium-bearing titanomagnetite at Hongge, China, accounts for 49.5% of the total reserve in Panxi region, China [2]. It is also widely recognized as the biggest chromium-bearing deposit in China [3]. At present, the titanomagnetite concentrates are smelted in the blast furnace to produce hot metal and blast furnace slag [3]. The blast furnace slag contains 22%−25% TiO_2 and 2%−6% metallic iron, and it is rather difficult to be efficiently utilized, resulting in resource depletion [4−6].

To efficiently recover titanium resources from vanadium-bearing titanomagnetite, coal-based direct reduction with subsequent electric furnace smelting has gained considerable attention as an alternative route to the conventional blast furnace process [7,8]. The molten

Foundation item: Projects (2013CB632601, 2013CB632604) supported by the National Basic Research Program of China; Project (51125018) supported by the National Science Foundation for Distinguished Young Scholars of China; Project (KGZD-EW-201-2) supported by the Key Research Program of the Chinese Academy of Sciences; Projects (51374191, 21106167, 51104139) supported by the National Natural Science Foundation of China

Corresponding author: Li-na WANG; Tel: +86-10-82544848; E-mail: linawang@ipe.ac.cn

DOI: 10.1016/S1003-6326(15)63731-1

iron obtained by electric furnace smelting is oxidized in BOF converter to produce vanadium slag. It is difficult to efficiently recover the vanadium and chromium by roasting−leaching process from the vanadium slag with stable spinel structure [9,10], and the residual hazardous compounds such as V(V) and Cr(VI) in the leaching residue inevitably pose a great threat to the environment [11].

Therefore, a new cleaner production process for the efficient utilization of high-chromium vanadium-bearing titanomagnetite concentrates has been proposed by ZHAO et al [12]. In this process, most of the vanadium and chromium are not reduced and concentrated in the titanium slag during direct reduction. After magnetic separation, vanadium and chromium can be efficiently extracted from the titanium slag using hydrometallurgical processes, so that converter smelting and roast-leach processes can be avoided. However, few studies have been focused on the reduction behaviors of vanadium and chromium in the titanomagnetite concentrates during direct reduction, which have a decisive impact on the elemental distribution of vanadium and chromium between iron concentrate and titanium slag during magnetic separation. Therefore, it is imperative to investigate the reduction behaviors of vanadium and chromium in the concentrates during coal-based direct reduction.

The objectives of the present work are to investigate the reduction behaviors of vanadium and chromium in the isothermal reduction of high-chromium vanadium-bearing titanomagnetite concentrates and their effects on the elemental distribution in the subsequent magnetic separation.

2 Experimental

2.1 Materials

The high-chromium vanadium-bearing titanomagnetite concentrates (<150 μm) used in this work were obtained from Hongge District, southwest China. The chemical composition of the titanomagnetite concentrates is given in Table 1. XRD analysis in Fig. 1 indicates that the titanomagnetite concentrates consist mostly of titanomagnetite (Fe_2TiO_4), with small amounts of ilmenite. The mineralogical investigation indicates that above 97% of the vanadium and chromium in the concentrates were embedded in the titanomagnetite, the octahedral sites of which were occupied by trivalent ions such as V(III) and Cr(III), forming $FeO{\cdot}(Fe,V,Cr)_2O_3$. The pulverized coal is used as a reductant (<150 μm), and the industrial analysis results are listed in Table 2.

2.2 Experimental procedures

The reduction experiments were conducted in a temperature controlled Muffle furnace with precise temperature (±1 °C) controls. The titanomagnetite concentrates (120 g) were firstly mixed homogenously with pulverized coal and 2.5% Na_2CO_3 additive. The presence of minor amounts of Na_2CO_3 largely facilitated the carbon gasification reaction and thereby exerted a positive influence on the reduction of the titanomegnetite concentrates, as well as induced the growth of the metallic phases probably because of the formation of a small amount of liquid phases [13−15]. The obtained mixtures were then placed in a capped SiC crucible and heated at various temperatures for 2 h. The crucible was not completely sealed to ensure that the inside pressure was almost equal to the atmospheric pressure. After reduction, the reduced samples were removed and immediately quenched with water to avoid re-oxidation, with subsequent crushing and grinding in a XMB-0.5L steel rod mill (Wuhan Exploring Machinery Factory, China) at ambient temperature for 30 min. The milling medium was made of hardened stainless steel rods.

The magnetic separation was conducted in a DTCXG-ZN50 low intensity magnetic separator (Tangshan DTEE Electrical Equipment Co., Ltd., China)

Table 1 Chemical composition of high-chromium vanadium-bearing titanomagnetite concentrates (mass fraction, %)

TFe	FeO	TiO_2	V_2O_5	Cr_2O_3
55.14	27.33	13.60	0.58	1.10

CaO	MgO	Al_2O_3	SiO_2
1.10	4.24	3.36	3.12

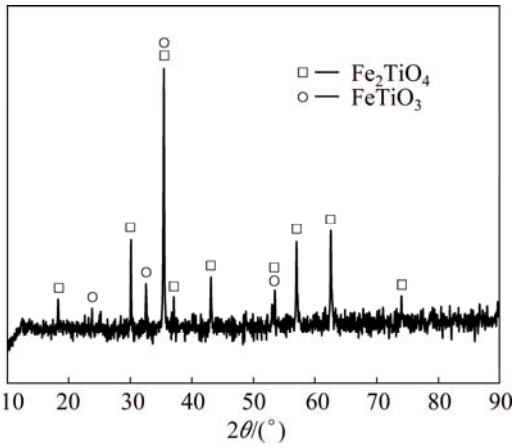

Fig. 1 XRD pattern of high-chromium vanadium-bearing titanomagnetite concentrates

Table 2 Industrial analysis results of pulverized coal (mass fraction, %)

FC_{ad}	V_{daf}	A_d	M_{ad}	S
87.10	4.07	8.83	2.08	0.376

FC_{ad}: Fixed carbon in air dried sample, V_{daf}: Volatiles in air dried sample, A_d: Ash in air dried sample, M_{ad}: Moisture in air dried sample

with a glass tube which was placed between the bobbins at an angle of 45°. The rod-milled samples were separated by a magnetic separator, with a magnetic field intensity of 48 kA/m. The obtained iron concentrate and titanium slag were then dried under the protection of nitrogen atmosphere.

The chemical compositions of the iron concentrate and titanium slag were analyzed using ICP-OES, and the recoveries of iron, titanium, vanadium, and chromium in the iron concentrate were calculated according to the mass balance.

2.3 Characterization

The chemical composition of samples was examined by ICP-OES (Optima 5300DV, Perkin Elmer, USA). The morphological characterization and compositional analyses of the samples were also performed by scanning electron microscopy (SEM) and energy dispersive spectroscopy (EDS). The mineral phases of samples were investigated by an X'Pert PRO MPD X-ray diffraction (XRD) using Cu K_α radiation running at 40 kV.

3 Results and discussion

3.1 Effect of *n*(C)/*n*(Fe)

The effect of *n*(C)/*n*(Fe) on the metallization degree and the recoveries of the metals during magnetic separation was investigated. The reduction experiments were conducted at 1200 °C for 2 h, and the results are depicted in Fig. 2.

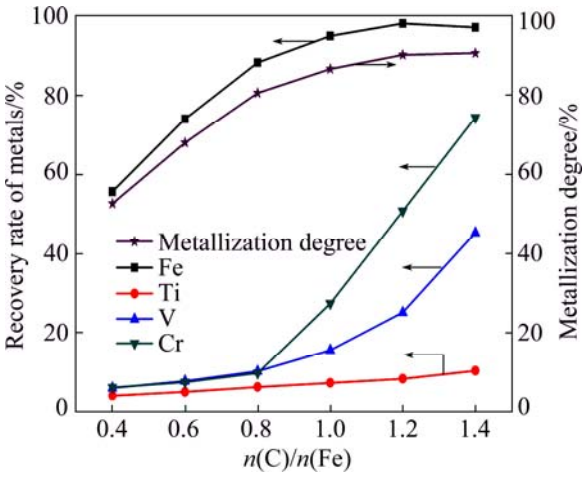

Fig. 2 Effect of *n*(C)/*n*(Fe) on metallization degree and recoveries of metals under conditions of temperature 1200 °C and time 2 h

As shown in Fig. 2, the metallization degree increased from 52.7% to 90.7% as the *n*(C)/*n*(Fe) increased from 0.4 to 1.4. The recovery of iron significantly increased from 55.7% to 88.3% as the *n*(C)/*n*(Fe) increased from 0.4 to 0.8, whereas the recoveries of titanium, vanadium and chromium remained relatively unchanged. With further increasing the *n*(C)/*n*(Fe), the recoveries of iron and titanium increased slightly, while the recoveries of vanadium and chromium rapidly increased from 10.0% and 9.6% to 45.3% and 74.3%, respectively. This may be attributed to the fact that *n*(C)/*n*(Fe) had a considerable impact on the reduction behaviors of $FeO{\cdot}V_2O_3$ and $FeO{\cdot}Cr_2O_3$, resulting in the difference in the recoveries of vanadium and chromium during magnetic separation.

To verify the above speculations, the element distribution maps and the micro-analyses of the samples reduced at different *n*(C)/*n*(Fe) values were performed. The sections of the samples were first polished, sputter-coated with gold, and then examined by SEM, using back-scattered electron imaging to yield atomic number contrast. The element distribution maps of the samples are shown in Fig. 3. The micro-analyses of the samples are listed in Table 3. At least five regions were analyzed per phase, and then the average chemical composition was calculated.

As shown in Fig. 3, iron mainly presented in the metallic iron phase (M), while titanium and vanadium mainly distributed in the Ti-rich phase (A). However, the phases where chromium presented changed from phase A to phase M as the *n*(C)/*n*(Fe) increased from 0.8 to 1.2. According to Table 3, with increasing the *n*(C)/*n*(Fe), the vanadium content of phase M increased slightly while that of phase A remained steadily. However, the chromium content of phase M increased rapidly as the *n*(C)/*n*(Fe) increased, whereas that of phase A decreased gradually. It might be deduced that chromium oxides were easier to be reduced than vanadium oxides during reduction. The titanium content of phase A largely increased as the *n*(C)/*n*(Fe) increased, while the iron content decreased rapidly. This may be attributed to the fact that iron oxides were reduced to metallic iron, while titanium oxides remained in the Ti-rich phase, causing obvious changes in the titanium and iron contents.

3.2 Effect of temperature (*n*(C)/*n*(Fe)=0.8)

The effect of temperature on the metallization degree and the recoveries of the metals was also investigated at the *n*(C)/*n*(Fe) of 0.8 and the time of 2 h. The results are shown in Fig. 4.

As seen in Fig. 4, the metallization degree gradually increased as the *n*(C)/*n*(Fe) increased. The recovery of iron increased gradually with increasing the temperature from 1000 °C to 1100 °C, whereas the recoveries of titanium, vanadium, and chromium decreased. It was accepted that higher temperatures favored the isothermal reduction and induced the grain growth of the newly

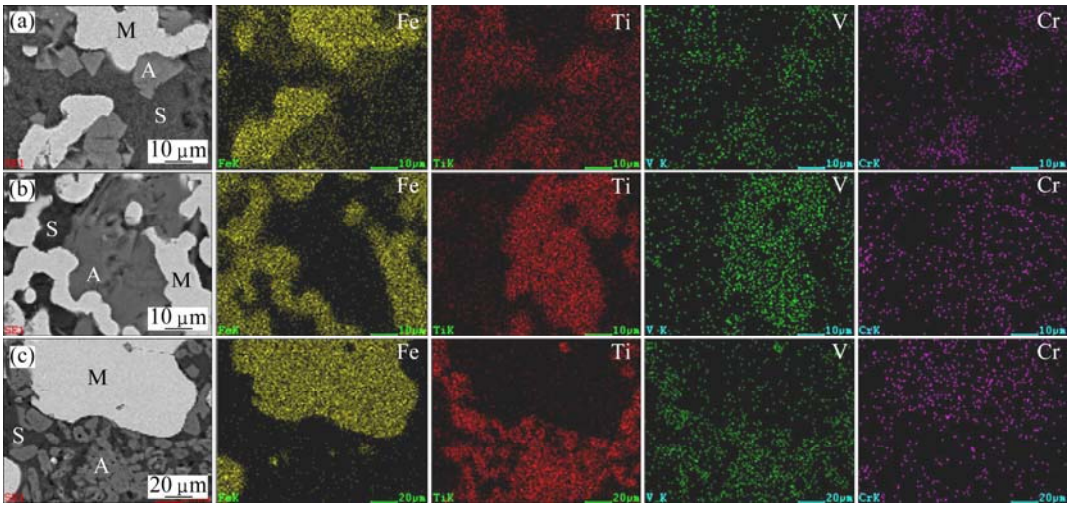

Fig. 3 SEM images and element distribution maps of samples reduced with *n*(C)/*n*(Fe) values of 0.8 (a), 1.0 (b), and 1.2 (c)

Table 3 Micro-analyses of samples reduced with different *n*(C)/*n*(Fe) values at 1200 °C for 2 h

n(C)/*n*(Fe) molar ratio	Mineral phase	Average mass fraction/%				
		Fe	Ti	V	Cr	C
0.8	Metallic iron (M)	98.90	0.64	0.15	0.22	0.09
	Ti-rich phase (A)	25.05	19.43	1.34	3.32	
	Silicates (S)	5.68	7.51	0.12	0.18	
1.0	Metallic iron (M)	98.35	0.89	0.20	0.41	0.46
	Ti-rich phase (A)	2.24	49.03	1.35	1.38	
	Silicates (S)	10.20	4.04	0.13	0.17	
1.2	Metallic iron (M)	97.33	0.75	0.28	1.15	1.19
	Ti-rich phase (A)	1.48	57.36	1.21	0.81	
	Silicates (S)	6.37	3.93	0.13	0.16	

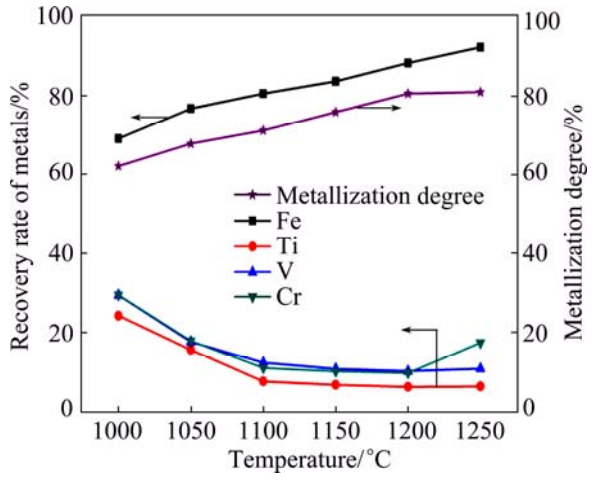

Fig. 4 Effect of temperature on metallization degree and recoveries of metals under conditions of *n*(C)/*n*(Fe) 0.8 and time 2 h

formed metallic iron, improving the efficiency of magnetic separation [16]. Afterwards, the recovery of iron continued to increase while those of titanium, vanadium, and chromium basically maintained steadily with the continued increase of the temperature. It was speculated that most of the $FeO{\cdot}V_2O_3$ and $FeO{\cdot}Cr_2O_3$ were not expected to be reduced at low *n*(C)/*n*(Fe) because of the lack of carbonaceous reductants.

To confirm the behaviors of vanadium and chromium, the element distribution maps and the micro-analyses of the samples reduced at different temperatures were studied. The element distribution maps of the samples are presented in Fig. 5. The micro-analyses of the samples are listed in Table 4.

As can be seen from Fig. 5, iron predominantly distributed in phase M, while titanium, vanadium, and chromium mainly presented in phase A in the temperature range of 1100−1250 °C. Table 4 indicated that the vanadium and chromium contents in phase M basically maintained steadily with increasing the temperature from 1100 °C to 1250 ℃, except for the slight increase of the chromium content at 1250 °C. This might be attributed to the formation of metallic chromium at temperatures higher than 1250 °C. These results also agreed very well with the results presented in Fig. 4.

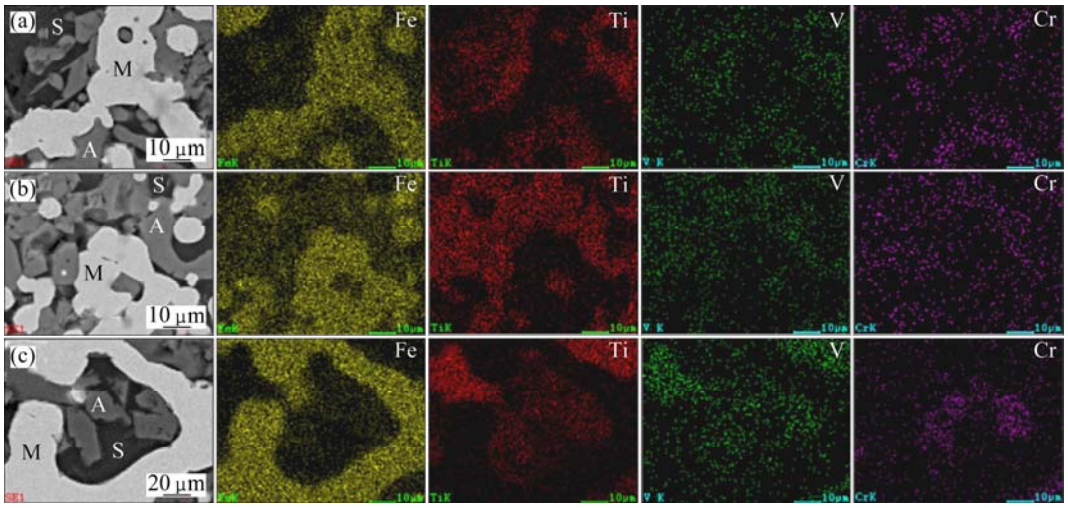

Fig. 5 SEM images and element distribution maps of samples reduced with n(C)/n(Fe) of 0.8 at 1100 °C (a), 1150 °C (b), and 1250 °C (c)

Table 4 Micro-analyses of samples reduced at different temperatures with n(C)/n(Fe) of 0.8 for 2 h

Temperature/°C	Mineral phase	Average mass fraction/%				
		Fe	Ti	V	Cr	C
1100	Metallic iron (M)	98.32	0.86	0.21	0.31	0.10
	Ti-rich phase (A)	31.14	17.37	0.73	1.65	
	Silicates (S)	10.56	6.35	0.10	0.23	
1150	Metallic iron (M)	98.25	0.98	0.21	0.29	0.09
	Ti-rich phase (A)	36.85	21.44	1.22	2.30	
	Silicates (S)	13.71	8.04	0.24	0.05	
1250	Metallic iron (M)	98.48	0.66	0.19	0.42	0.11
	Ti-rich phase (A)	5.35	49.07	1.52	1.23	
	Silicates (S)	6.81	6.96	0.12	0.26	

3.3 Effect of temperature (n(C)/n(Fe) = 1.2)

The effect of temperature on the metallization degree and the recoveries of the metals was also investigated with the n(C)/n(Fe) molar ratio of 1.2 and the time of 2 h, as seen in Fig. 6.

Figure 6 shows that the metallization degree increased slowly as the temperature increased. The recovery of iron increased considerably with increasing the temperature from 1000 °C to 1100 °C, while those of titanium, vanadium, and chromium decreased. With further increasing the temperature to 1200 °C, the recoveries of vanadium and chromium increased gradually, while that of titanium decreased slightly. Further increase in the temperature caused sharp increase in the recoveries of vanadium and chromium. It may be attributed to the different reduction behaviors of $FeO{\cdot}V_2O_3$ and $FeO{\cdot}Cr_2O_3$ at higher n(C)/n(Fe).

The element distribution maps and the micro-analyses of the samples reduced at various temperatures were studied to confirm the behaviors of vanadium and chromium during magnetic separation. The element distribution maps and the micro-analyses of the samples were presented in Fig. 7 and Table 5, respectively.

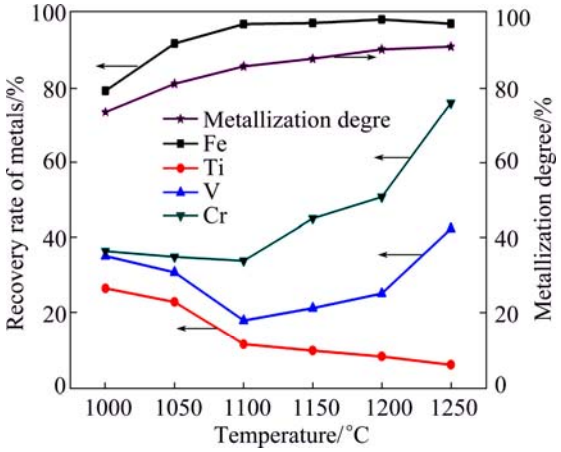

Fig. 6 Effect of temperature on metallization degree and recoveries of metals under conditions of n(C)/n(Fe) 1.2 and time 2 h

As shown in Fig. 7, iron mainly presented in phase

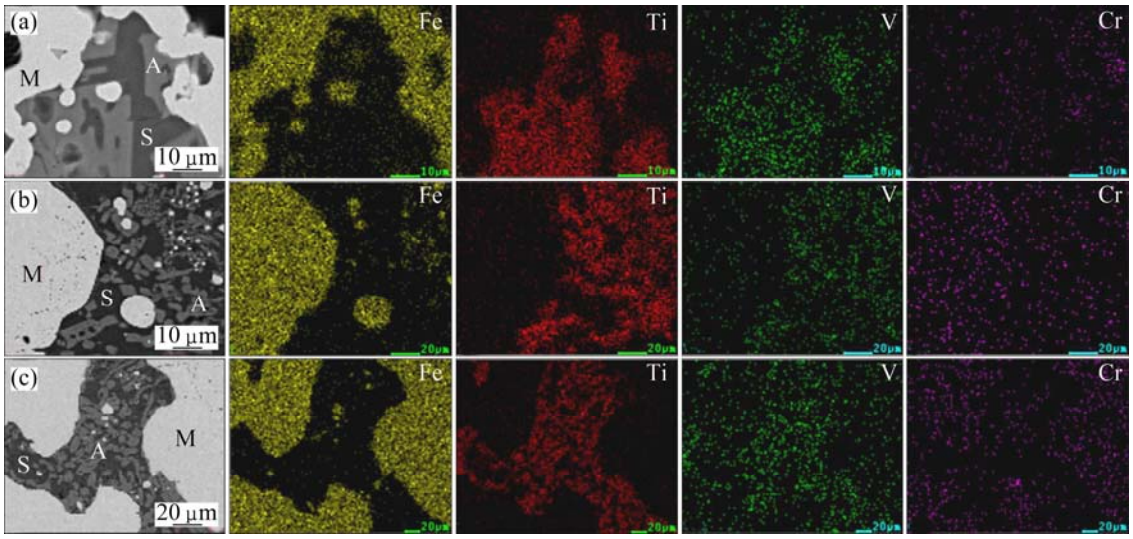

Fig. 7 SEM images and element distribution maps of samples reduced with n(C)/n(Fe) of 1.2 at 1100 °C (a), 1150 °C (b), and 1250 °C (c)

Table 5 Micro-analyses of samples reduced at different temperatures with n(C)/n(Fe) of 1.2 for 2 h

Temperature/°C	Mineral phase	Average mass fraction/%				
		Fe	Ti	V	Cr	C
1100	Metallic iron (M)	98.26	0.57	0.23	0.62	1.29
	Ti-rich phase (A)	2.11	47.70	1.30	1.72	
	Silicates (S)	2.73	6.74	0.22	0.58	
1150	Metallic iron (M)	97.68	0.70	0.35	0.93	1.18
	Ti-rich phase (A)	1.19	49.25	1.32	1.13	
	Silicates (S)	1.06	3.07	0.18	0.39	
1250	Metallic iron (M)	97.81	0.32	0.44	1.32	1.08
	Ti-rich phase (A)	1.24	54.65	1.03	0.79	
	Silicates (S)	0.58	5.68	0.08	0.20	

M, while titanium predominantly distributed in phase A. As the temperature increased from 1100 °C to 1250 °C, vanadium predominantly distributed in phase A, while the chromium-enriched phases changed from phase A to phase M. The results in Table 5 show that the vanadium content in phase M increased slightly as the temperature raised while the chromium content increased rapidly. These results further confirmed the results presented in Fig. 6.

3.4 Reduction behaviors of titanomagnetite concentrates

3.4.1 Thermodynamic analysis

As noted above, the titanomagnetite concentrates consisted mostly of titanomagnetite (Fe_2TiO_4), and the vanadium and chromium existed in the forms of $FeO{\cdot}V_2O_3$ and $FeO{\cdot}Cr_2O_3$, respectively. During coal-based direct reduction, carbon monoxide (CO) was more effective than solid carbon [17]. Assuming that the Boudouad reaction reached equilibrium in the temperature range of 1100−1600 K, the Gibbs free energy changes (ΔG, kJ/mol) of the possible reduction reactions of the titanomagnetite concentrates were calculated according to the thermochemical data of pure substances [18] and listed as follows.

Boudouad reaction:

$$CO_2+C=2CO,\ \Delta G=\Delta G^{\Theta}+RT\ln[(p_{CO})^2/(p_{CO_2}\cdot p^{\Theta})]=0 \quad (1)$$

Reduction of titanomagnetite:

$$Fe_2TiO_4+CO=Fe+FeTiO_3+CO_2,\ \Delta G=155.24-0.143T \quad (2)$$

$$Fe_2TiO_4+2CO=2Fe+TiO_2+2CO_2,\ \Delta G=333.46-0.299T \quad (3)$$

$$2Fe_2TiO_4+MgO+4CO=4Fe+MgTi_2O_5+4CO_2,\ \Delta G=637.45-0.605T \quad (4)$$

$$3Fe_2TiO_4+7CO=6Fe+Ti_3O_5+7CO_2,\ \Delta G=-252.52-0.782T \quad (5)$$

Reduction of $FeO·V_2O_3$:

$$FeO·V_2O_3+CO=Fe+V_2O_3+CO_2,$$
$$\Delta G=164.84-0.147T \quad (6)$$

$$FeO·V_2O_3+2CO=Fe+2VO+2CO_2,$$
$$\Delta G=399.74-0.309T \quad (7)$$

$$FeO·V_2O_3+4CO=Fe+2V+4CO_2,$$
$$\Delta G=1003.88-0.630T \quad (8)$$

$$FeO·V_2O_3+7.52CO=Fe+2VC_{0.88}+5.76CO_2,$$
$$\Delta G=806.13-0.621T \quad (9)$$

Reduction of $FeO·Cr_2O_3$:

$$FeO·Cr_2O_3+CO=Fe+Cr_2O_3+CO_2,$$
$$\Delta G=205.23-0.162T \quad (10)$$

$$FeO·Cr_2O_3+4CO=Fe+2Cr+4CO_2,$$
$$\Delta G=975.03-0.662T \quad (11)$$

$$7FeO·Cr_2O_3+40CO=7Fe+2Cr_7C_3+34CO_2,$$
$$\Delta G=6521.75-4.707T \quad (12)$$

According to the thermodynamic calculation, Fe_2TiO_4 is easier to be reduced by CO than $FeO·V_2O_3$ and $FeO·Cr_2O_3$. Metallic chromium and vanadium were formed at temperatures higher than 1200 °C and 1320 °C, respectively. However, vanadium and chromium carbides were formed at much lower temperatures.

3.4.2 Reduction behavior of titanomagnetite based on XRD analysis

The influence of temperature (1000−1250 °C) on the phase transformation during reduction was investigated with the reduction time of 2 h. The results are shown in Fig. 8.

As shown in Fig. 8, titanomagnetite was gradually reduced to metallic iron, ilmenite and pseudobrookite when the temperature was raised, which agreed very well with the former researches [17,19]. At the n(C)/n(Fe) of 0.8, titanomagnetite and ilmenite still existed in the reduced samples even when the temperature was raised to 1250 °C, probably because of the lack of reductants. Thus, Reactions (2) and (4) occurred but proceeded incompletely. At the n(C)/n(Fe) of 1.2, titanomagnetite and ilmenite were completely reduced, and the main phases of the final reduced sample were metallic iron and pseudobrookite. Therefore, Reactions (2) and (4) proceeded completely, and Reaction (5) probably occurred.

3.4.3 Reduction behaviors of $FeO·V_2O_3$ and $FeO·Cr_2O_3$

According to Table 3, the carbon content of phase M increased with increasing the n(C)/n(Fe). This might be partially attributed to the fact that vanadium and chromium are strong carbide-forming elements [20,21]. The formation of vanadium and chromium carbides was largely induced by increasing the n(C)/n(Fe). In the Fe−C binary system, austenite with face-centered cubic structure (γ(FCC)) occurred in the Fe-rich regions at around 1200 °C [22]. The minor amount of newly-formed carbides were then dissolved in the metallic iron, forming γ(FCC) phase [20,21,23], resulting in the increase of the recoveries during magnetic separation.

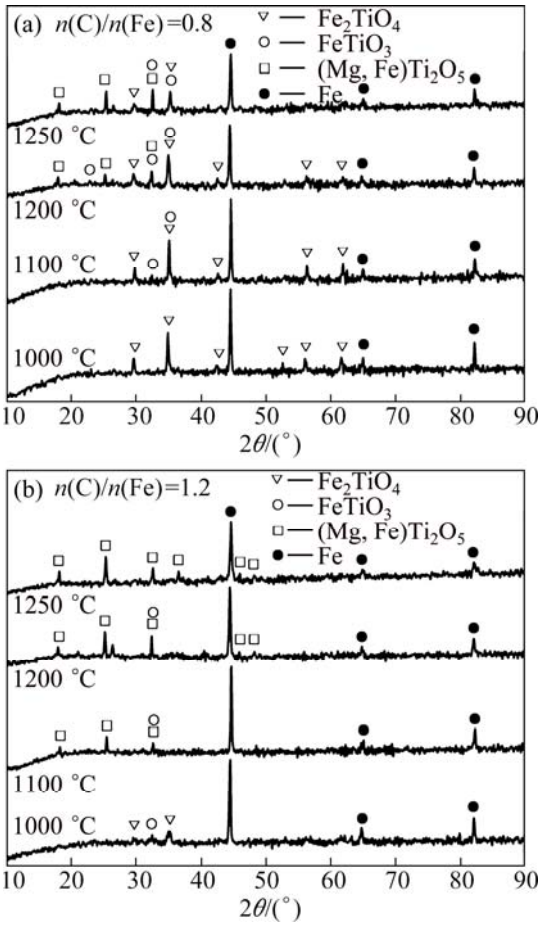

Fig. 8 XRD patterns of reduced samples under different conditions

At the n(C)/n(Fe) of 0.8, the carbon content of phase M remained unchangeable (~0.1%) as the temperature was raised (Table 4). Thus, it was accepted that few carbides were formed because of the lack of carbonaceous reductants. In this regard, Reactions (2), (4), (6), (7), and (10) occurred at the n(C)/n(Fe) of 0.8. Nevertheless, metallic chromium was expected to be formed at 1250 °C according to Reaction (11), resulting in the slight increase in the chromium recovery (Fig. 4). As shown in Table 5, the carbon contents of phase M were higher than 1.0% in the temperature range of 1100−1250 °C because of the formation of minor amount of carbides. This could be attributed to the fact that higher temperatures induced the dissolution of vanadium and chromium carbides into the γ(FCC) phase in the

temperature range of 1100−1250 °C [20−24]. Thus, Reactions (2)−(7), (9), (10), and (12) occurred at the n(C)/n(Fe) of 1.2. Furthermore, Reaction (11) occurred when the temperature was raised to 1250 °C. These results further confirmed the above analysis on the reduction behaviors of $FeO{\cdot}V_2O_3$ and $FeO{\cdot}Cr_2O_3$.

4 Conclusions

1) The reduction behaviors of $FeO{\cdot}V_2O_3$ and $FeO{\cdot}Cr_2O_3$ in the high-chromium vanadium-bearing titanomagnetite concentrates were largely influenced by the n(C)/n(Fe). The recoveries of vanadium and chromium rapidly increased from 10.0% and 9.6% to 45.3% and 74.3%, respectively, as the n(C)/n(Fe) increased from 0.8 to 1.4.

2) At the n(C)/n(Fe) of 0.8, the recoveries of vanadium and chromium are always lower than 10.0% in the whole temperature range of 1100−1250 °C. This could be attributed to the fact that most of the $FeO{\cdot}V_2O_3$ and $FeO{\cdot}Cr_2O_3$ were not reduced to carbides even if the temperature rose to 1250 °C because of the lack of carbonaceous reductants.

3) At the n(C)/n(Fe) of 1.2, the recoveries of vanadium and chromium considerably increased from 17.8% and 33.8% to 42.4% and 76.0%, respectively, as the temperature increased from 1100 °C to 1250 °C. This could be explained by the fact that $FeO{\cdot}V_2O_3$ and $FeO{\cdot}Cr_2O_3$ could be reduced to carbides because of the excess amount of carbonaceous reductants, and the formation of carbides was largely induced by increasing temperature. The newly formed carbides were then dissolved in the γ(FCC) phase, causing a rapid increase in the recoveries of vanadium and chromium during magnetic separation.

References

[1] TAYLOR P R, SHUEY S A, VIDAL E E, GOMEZ J C. Extractive metallurgy of vanadium-containing titaniferous magnetite ores: A review [J]. Minerals and Metallurgical Processing, 2006, 23: 80−86.

[2] TAN Qi-you, CHEN Bo, ZHANG Yu-shu, LONG Yun-bo, YANG Yao-hui. Characteristics and current situation of comprehensive utilization of vanadium titanomagnetite resources in Panxi region [J]. Multipurpose Utilization of Mineral Resources, 2011, 6: 6−10. (in Chinese)

[3] DU He-gui. Theory of smelting vanadium-bearing titanomagnetite by blast furnace [M]. Beijing: Science Press, 1996: 1−17. (in Chinese)

[4] CHEN De-sheng, ZHAO Long-sheng, QI Tao, HU Guo-ping, ZHAO Hong-xin, LI Jie, WANG Li-na. Desilication from titanium-vanadium slag by alkaline leaching [J]. Transactions of Nonferrous Metals Society of China, 2013, 23(10): 3076−3082.

[5] CHEN De-sheng, SONG Bo, WANG Li-na, QI Tao, WANG Yong, WANG Wei-jing. Solid state reduction of Panzhihua titanomagnetite concentrates with pulverized coal [J]. Minerals Engineering, 2011, 24: 864−869.

[6] SUN Hao-yan, DONG Xiang-juan, SHE Xue-feng, XUE Qing-guo, WANG Jing-song. Solid state reduction of titanomagnetite concentrate by graphite [J]. ISIJ International, 2013, 53: 564−569.

[7] ZHOU Lan-hua, ZENG Fu-hong. Reduction mechanisms of vanadium− titanomagnetite−non-coking coal mixed pellet [J]. Ironmaking and Steelmaking, 2011, 38: 59−64.

[8] ROSHCHIN V E, ASANOV A V, ROSHCHIN A V. Possibilities of two-stage processing of titaniferous magnetite ore concentrates [J]. Russian Metallurgy (Metally), 2011, 6: 499−508.

[9] WANG Zhong-hang, ZHENG Shi-li, WANG Shao-na, LIU Biao, WANG Da-wei, DU Hao, ZHANG Yi. Research and prospect on extraction of vanadium slag by liquid oxidation technologies [J]. Transactions of Nonferrous Metals Society of China, 2014, 24: 1273−1288.

[10] LIU Biao, DU Hao, WANG Shao-na, ZHANG Yi, ZHENG Sheng-li, LI Lan-jie, CHEN D H. A novel method to extract vanadium and chromium from vanadium slag using molten $NaOH$-$NaNO_3$ binary system [J]. AIChE Journal, 2013, 59: 541−552.

[11] MAYES W M, YOUNGER P L, AUMONIER J. Hydrogeochemistry of alkaline steel slag leachates in the UK [J]. Water, Air, and Soil Pollution, 2008, 195: 35−50.

[12] ZHAO Long-sheng, WANG Li-na, QI Tao, CHEN De-sheng, ZHAO Hong-xin, LIU Ya-hui. A novel method to extract iron, titanium, vanadium, and chromium from high-chromium vanadium-bearing titanomagnetite concentrates [J]. Hydrometallurgy, 2014, 149: 106−109.

[13] BASUMALLICK A. Influence of CaO and Na_2CO_3 as additive on the reduction of hematite-lignite mixed pellets [J]. ISIJ International, 1995, 35: 1050−1053.

[14] HUANG Zhu-cheng, CAI Ling-bo, ZHANG Yuan-bo, YANG Yong-bin, JIANG Tao. Reduction of iron oxides of red mud reinforced by Na_2CO_3 and CaF_2 [J]. Journal of Central South University (Science and Technology), 2010, 41: 838−844. (in Chinese)

[15] ZHOU Lan-hua, ZENG Fu-hong. Statistical analysis of the effect of Na_2CO_3 as additive on the reduction of vanadic-titanomagnetite-coal mixed pellets [J]. Advanced Materials Research, 2010, 97−101: 465−470.

[16] WEISSBERGER S, ZIMMELS Y, LIN I J. Mechanism of growth of metallic phase in direct reduction of iron bearing oolites [J]. Metallurgical Transactions B, 1986, 17: 433−442.

[17] HU Tu, LV Xue-wei, BAI Chen-guang, LUN Zhi-gang, QIU Gui-bao. Reduction behavior of Panzhihua titanomagnetite concentrates with coal [J]. Metallurgical and Materials Transactions B, 2013, 44: 252−260.

[18] BARIN I. Thermochemical data of pure substances [M]. 3rd ed. Weinheim: VCH Verlag GmbH, 1995: 209−1778.

[19] PARK E, OSTROVSKI O. Effects of preoxidation of titania-ferrous ore on the ore structure and reduction behavior [J]. ISIJ International, 2004, 44: 74−81.

[20] BRATBERG J, FRISK K. An experimental and theoretical analysis of the phase equilibria in the Fe−Cr−V−C system [J]. Metallurgical and Materials Transactions A, 2004, 35, 3649−3663.

[21] LEE B J, LEE D N. A thermodynamic evaluation of the Fe−Cr−V−C system [J]. Journal of Phase Equilibria, 1992, 13: 349−364.

[22] CHIPMAN J. Thermodynamics and phase diagram of the Fe−C system [J]. Metallurgical Transactions, 1972, 3: 55−64.

[23] VILLARS P, PRINCE A, OKAMOTO H. Handbook of ternary alloy phase diagrams [M]. 2nd ed. Geauga, Ohio: ASM International, 1995: 1548−1950.

[24] WADA T, WADA H, ELLIOTT J F, CHIPMAN J. Activity of carbon and solubility of carbides in the FCC Fe−Mo−C, Fe−Cr−C, and Fe−V−C alloys [J]. Metallurgical Transactions, 1972, 3: 2865−2872.

高铬型钒钛磁铁精矿煤基直接还原–磁选分离过程中钒和铬的行为

赵龙胜[1,2,3]，王丽娜[2,3]，陈德胜[2,3]，赵宏欣[2,3]，刘亚辉[2,3]，齐 涛[2,3]

1. 中国科学院大学，北京 100049；
2. 中国科学院 过程工程研究所 湿法冶金清洁生产技术国家工程实验室，北京 100190；
3. 中国科学院 过程工程研究所 绿色过程与工程院重点实验室，北京 100190

摘 要：高铬型钒钛磁铁精矿的煤基直接还原过程中 $FeO·V_2O_3$ 和 $FeO·Cr_2O_3$ 的还原行为对其高效综合利用产生决定性的影响。采用 XRD、SEM 及 EDS 等手段对直接还原产物进行分析，分别考察碳铁摩尔比和温度对煤基直接还原–磁选分离过程中钒和铬行为的影响。结果表明：当碳铁摩尔比(n(C)/n(Fe))从 0.8 增大到 1.4 时，V 和 Cr 的回收率分别从 10.0%和 9.6%增大到 45.3%和 74.3%。当 n(C)/n(Fe)为 0.8 时，在 1100~1250 °C 的温度范围内，V 和 Cr 的回收率始终低于 10.0%；而当 n(C)/n(Fe)为 1.2 时，随着温度从 1100 °C 升高到 1250 °C，V 和 Cr 的回收率分别从 17.8%和 33.8%增大到 42.4%和 76.0%。当 n(C)/n(Fe)低于 0.8 时，由于含碳还原剂的量不足，绝大多数 $FeO·V_2O_3$ 和 $FeO·Cr_2O_3$ 不能被还原成碳化物，且温度(1100~1250 °C)对其还原行为的影响甚微。在更高的 n(C)/n(Fe)下，由于含碳还原剂的量充足，$FeO·V_2O_3$ 和 $FeO·Cr_2O_3$ 的还原率大幅提高，且更高的温度能有效地促进碳化物的生成。新生成的碳化物溶解在 γ(FCC)相中，并在磁选过程中与金属铁同时回收。

关键词：高铬型钒钛磁铁精矿；煤基直接还原；磁选分离；还原行为；钒；铬

(Edited by Yun-bin HE)